Stromal Transcription Factor 21 Regulates Development of the Renal Stroma *via* Interaction with Wnt/β-Catenin Signaling

Gal Finer [1,2,3] Yoshiro Maezawa [4] Shintaro Ide [5] Tuncer Onay [2,6] Tomokazu Souma [5] Rizaldy Scott [2,6] Xiaoyan Liang,[1,3] Xiangmin Zhao,[1] Gaurav Gadhvi [7] Deborah R. Winter [7] Susan E. Quaggin,[2,6] and Tomoko Hayashida [1,3]

Key Points

- Transcription factor 21 in Foxd1+ interstitial progenitors is required for proliferation and differentiation of the renal stroma.
- Tcf21 binds to β-catenin and enhances expression of stromal Wnt target genes.
- The kidney stroma is critical for normal development of the nephron progenitor cells, loop of Henle, and collecting ducts.

Abstract

Background Kidney formation requires coordinated interactions between multiple cell types. Input from the interstitial progenitor cells is implicated in multiple aspects of kidney development. We previously reported that transcription factor 21 (Tcf21) is required for ureteric bud branching. Here, we show that Tcf21 in Foxd1+ interstitial progenitors regulates stromal formation and differentiation *via* interaction with β-catenin.

Methods We utilized the Foxd1Cre;Tcf21$^{f/f}$ murine kidney for morphologic analysis. We used the murine clonal mesenchymal cell lines MK3/M15 to study Tcf21 interaction with Wnt/β-catenin.

Results Absence of Tcf21 from Foxd1+ stromal progenitors caused a decrease in stromal cell proliferation, leading to marked reduction of the medullary stromal space. Lack of Tcf21 in the Foxd1+ stromal cells also led to defective differentiation of interstitial cells to smooth-muscle cells, perivascular pericytes, and mesangial cells. Foxd1Cre;Tcf21$^{f/f}$ kidney showed an abnormal pattern of the renal vascular tree. The stroma of Foxd1Cre;Tcf21$^{f/f}$ kidney demonstrated marked reduction in β-catenin protein expression compared with wild type. Tcf21 was bound to β-catenin both upon β-catenin stabilization and at basal state as demonstrated by immunoprecipitation *in vitro*. In MK3/M15 metanephric mesenchymal cells, Tcf21 enhanced TCF/LEF promoter activity upon β-catenin stabilization, whereas DNA-binding deficient mutated Tcf21 did not enhance TCF/LEF promoter activity. Kidney explants of Foxd1Cre;Tcf21$^{f/f}$ showed low mRNA expression of stromal Wnt target genes. Treatment of the explants with CHIR, a Wnt ligand mimetic, restored Wnt target gene expression. Here, we also corroborated previous evidence that normal development of the kidney stroma is required for normal development of the Six2+ nephron progenitor cells, loop of Henle, and the collecting ducts.

Conclusions These findings suggest that stromal Tcf21 facilitates medullary stroma development by enhancing Wnt/β-catenin signaling and promotes stromal cell proliferation and differentiation. Stromal Tcf21 is also required for the development of the adjacent nephron epithelia.

KIDNEY360 3: 1228–1241, 2022. doi: https://doi.org/10.34067/KID.0005572021

Introduction

Kidney development relies on interactions between the metanephric mesenchyme (MM) and the ureteric bud (1). The MM consists of at least three progenitor cell populations: the nephron progenitor cells (NPC), the forkhead box D1 (Foxd1+) cells, and the endothelial progenitors (2). The Six2+/Cited1+ NPC comprise the cap mesenchyme (CM) and undergo mesenchymal-to-epithelial transition to form the glomerulus, proximal tubule, loop of Henle, distal tubule, and connecting

[1]Division of Nephrology, Ann and Robert H. Lurie Children's Hospital of Chicago, Chicago, Illinois
[2]Feinberg Cardiovascular and Renal Research Institute, Northwestern University Feinberg School of Medicine, Chicago, Illinois
[3]Department of Pediatrics, Northwestern University Feinberg School of Medicine, Chicago, Illinois
[4]Department of Endocrinology, Hematology and Gerontology, Chiba University Graduate School of Medicine, Chiba, Japan
[5]Department of Medicine, Duke University, Durham, North Carolina
[6]Division of Nephrology/Hypertension, Northwestern University Feinberg School of Medicine, Chicago, Illinois
[7]Division of Rheumatology, Northwestern University Feinberg School of Medicine, Chicago, Illinois

Correspondence: Dr. Gal Finer MD, PhD, Division of Nephrology, Ann and Robert H. Lurie Children's Hospital of Chicago, 225 E. Chicago Avenue, Box 37 Chicago, IL 60611-2605. Email: gfiner@luriechildrens.org

segment (3,4). The Foxd1+ cells are a distinct progenitor cell population within the MM. The Foxd1+ cells surround the CM and give rise to a significant portion of the stroma, the renal capsule, the glomerular mesangium, and the mural cells of the renal arterial tree: renin-secreting cells, smooth-muscle cells, perivascular fibroblasts, and pericytes (5–8). Although the definition of the renal stroma remains broad, it is generally accepted that the stroma encompasses all of the non-endothelial and non-epithelial cells of kidney. In addition to being a structural scaffold to the kidney, the interstitium plays an important role in branching morphogenesis, in the balance between self-renewal and differentiation of the NPC, and in the development of the renal vasculature. Recent analysis suggests that the Foxd1+ interstitial progenitor population is heterogeneous and consists of at least three transcriptomically distinct cell types that give rise to at least 12 anatomically distinct stromal zones along the cortical-medullary axis of the kidney (9). The study also suggested that patterning of the nephron appears to be regulated by instructive signals sent by a specific stromal zone to an adjacent epithelial segment. However, the mechanisms by which the interstitium orchestrates its various functions remain poorly understood.

Cell type-specific basic helix-loop-helix (bHLH) transcription factors are key regulators of organ morphogenesis (10–13). Transcription factor 21 (also known as Pod1/capsulin/epicardin) is a class 2, mesoderm-specific, bHLH transcription factor that is expressed in mesenchyme-derived tissues, such as the lung, gut, gonad, and epicardium. In the kidney, Tcf21 is expressed in the mesenchyme surrounding the invading ureteric bud in both the Six2+ and Foxd1+ cells, beginning on embryonic day 10.5 (14). Tcf21 expression was found to be low in stillborn infants with renal dysplasia (15). Tcf21 has also been shown to be involved in coronary artery disease (10,11) and podocyte differentiation (12). Tcf21 functions as tumor suppressor as well (13,16). We previously showed that stroma-specific Tcf21 knockout (KO) mice (Foxd1-eGFPCre;Tcf21$^{f/f}$) demonstrate defective collecting duct development and consequent abnormal urine concentration capacity (17). We therefore set out to examine if Tcf21 in interstitial progenitors plays a role in stromal development.

Materials and Methods
Mice and Genotyping

All murine experiments were approved by the Animal Care Committee at the Center for Comparative Medicine of Northwestern University (Evanston, IL) and were performed in accordance with institutional guidelines and the National Institutes of Health Guide for the Care and Use of Laboratory Animals. *Tcf21$^{flox/floxf}$* and *Tcf21-LacZ* mice were created as previously described (18). The *Six2-eGFPCre* and *Foxd1-eGFPCre* mice were kind gifts from Dr. Andrew McMahon (University of Southern California, Los Angeles, CA) and are described elsewhere (4,6). Genotyping was performed with Quick-Load Taq 2× Master Mix (M0271L; New England Biolabs, Ipswich, MA), on 2% agarose gel for the PCR bands. Primer information is provided in Supplemental Table 1.

Histology, Immunohistochemistry, and Immunofluorescence

Murine embryo dissections were performed at the indicated time points. Samples were fixed with 10% neutral buffered formalin or 4% paraformaldehyde overnight, embedded in paraffin, and sectioned into 5 μm by the Mouse Histology and Phenotyping Laboratory of Northwestern University. Sections were deparaffinized in xylene and ethanol, and boiled in citrate buffer for antigen retrieval. Sections were then treated with 1% donkey serum with 0.3% Triton X-100 in PBS for 30 minutes at room temperature before incubating with primary antibodies at 4°C overnight. Sections were washed in PBS and incubated with Alexa Fluor fluorescence-conjugated secondary antibodies for 45 minutes at room temperature. Antibody information is as follows: LEF1 (2230s; Cell Signaling Technology, Danvers, MA), Krt8 (TROMA-I-s; Developmental Studies Hybridoma Bank, Iowa City, IA), Acta2 (A2547; Sigma–Aldrich, St. Louis, MO), PDGFRβ (ab32570; Abcam, Cambridge, United Kingdom), Six2 (11562–1-AP; Proteintech, Rosemont, IL), ECAD (AF748; R&D Systems, Minneapolis, MN), β-catenin (ab2365; Abcam), GFP (A11122; Life Technologies, Carlsbad, CA), Pbx1 (4342S; Cell Signaling Technology), Meis2 (ab73164; Abcam), uromodulin (THP; BT-590; Biomedical Technologies, Stoughton, MA), aquaporin2 (sc-9882; Santa Cruz Biotechnology, Santa Cruz, CA), and Ki67 (RM-9106; Thermo Fisher Scientific, Waltham, MA). All secondary antibodies were purchased from Molecular Probes Thermo Fisher Scientific and used at a 1:1000 dilution. For five-channel imaging, secondary antibodies were employed as follows: AlexaFluor 488, 555, 594, 647, and DAPI.

Quantification of Vessel Number, Wall Thickness, and Vessel Size

Cryo-sections (10 μm) of control (Foxd1Cre;Tcf21$^{f/f}$ or Foxd1Cre;Tcf21$^{f/+}$) and mutant (Foxd1Cre;Tcf21$^{f/f}$) were immunostained for Acta2 (A2547; Sigma–Aldrich). After image capturing, quantifications of Acta2+ area and total kidney area were measured with Fiji Image J-Win64 software. The ratio of Acta2-stained area over total kidney area was then calculated. All blood vessels in the coronal mid-cross-section were examined and counted. Vessel thickness was calculated as the difference between interior and exterior vessel diameter, which were measured with Fiji Image J-Win64. Vessel size was calculated by measuring the exterior vessel diameter.

Quantification of Glomeruli, Capillary Loops, and Perivascular Cells

E16.5 and E18.5 murine embryo paraffin sections were stained with CD31 (AF3628; R&D Systems) and CD146 (ab75769; Abcam). After image capturing, the glomeruli were recognized and counted independently by two blinded individuals. The size of the glomeruli and the number of glomerular capillary loops were measured with Fiji Image J-Win64 software. Nuclei of CD146+ cells around interlobular (*i.e.*, corticoradial) arteries, and CD146+ glomerular mesangial cells of control and mutant kidneys were selected, counted, and analyzed. Fluorescence intensity of

CD146 staining was measured using Fiji Image J. For arterial size, the maximal, minimal arterial diameters were measured with Fiji ImageJ.

Vascular Tracing

E16.5 murine embryo coronal mid-cross-sections stained with CD31 (AF3628; R&D Systems) were selected. CD31 staining pattern in the medulla of control and mutant kidneys was traced manually using PowerPoint scribble tool. Individual CD31 tracings were stacked together to illustrate the vascular pattern.

Tissue Clearing

E12.5/E13.5 murine kidneys were dissected, stained, and cleared according to Cui *et al.* (19). The tissue was cleared with BABB: one part benzyl alcohol (305197; Sigma–Aldrich) to two parts benzyl benzoate (W213802; Sigma–Aldrich). Samples were stained with anti-ACTA2 antibody (A2547; Sigma–Aldrich), anti-Krt8 Antibody (TROMA-1; Developmental Studies Hybridoma Bank), and anti-β-catenin antibody (ab2365; Abcam).

Isolation of Murine Kidney Fibroblasts

For isolation of murine kidney fibroblasts, *FoxD1-eGFP-Cre; Tcf21^{f/f}; mTmG* or *FoxD1-eGFPCre; mTmG* mice were used. Murine kidneys were perfused with PBS, and the kidneys were harvested. Kidneys were dissociated with a Multi-Tissue Dissociation Kit 2 and Gentle MACS dissociator (Miltenyi Biotec, Bergisch Gladbach, Germany) at 37°C for 30 minutes, following the program "Multi E." The digested samples were filtrated through 100-, 50-, 40-, and 30-μm strainers before FACS. For fibroblast cells, GFP+ cells were sorted with a SH800 FACS cell sorter (Sony Biotechnology, San Jose, CA).

Cell Surface Area and Cell Growth Assay

$Tcf21^{-/-}$ and $Tcf21^{+/+}$ fibroblast cells were seeded at 2×10^5 in six-well plates at 37°C in DMEM with 10% FBS and non-essential amino acids (Thermo Fisher Scientific). The plates were inserted in Incucyte C3 (Essen BioScience, Ann Arbor, MI) and imaged every hour for 24 hours. Cell surface area and growth rate were calculated by the Incucyte software.

RNA Isolation, cDNA Synthesis, and Real-Time PCR

Kidneys were dissected and preserved at –80°C after being snap-frozen in liquid nitrogen. Total RNA was extracted using the RNeasy Mini kit (74104; Qiagen, Valencia, CA). Reverse transcription was performed using the Iscript cDNA Synthesis Kit (1708891; Bio-Rad Laboratories, Hercules, CA). Quantitative RT-PCR was performed using iTaqTM Universal SYBR Green Supermix (6432474; Bio-Rad Laboratories). Data were analyzed as the ratio to GAPDH or S18. Primer information is provided in Supplemental Table 1.

Cell Culture, Plasmid Transfection, and Lithium Chloride Activation

The renal mesenchymal cells MK3 and M15 were kind gifts from Dr. Seppo Vanio (University of Oulu, Oulu, Finland) and Dr. Peter Hohenstein (Leiden University, Leiden,

Netherlands) respectively. Cells were cultured in DMEM with L-glutamine supplemented with 10% FBS, 100 μg/ml penicillin and 100 μg/ml streptomycin. In some experiments, cells were treated with lithium chloride (LiCl$_2$ L9650–100G; Sigma–Aldrich). Transfection was carried out using the Electroporation and Nucleofector Technology system (VCA-1003; Lonza, Basel, Switzerland). The following plasmids were used: Tcf21_eGFP empty vector (PEGFP-N1, 6085–1; Addgene, Watertown, MA), Tcf21 eGFP mutant and wild type (WT) generated and validated in our laboratory. Plasmid (2 μg; 1 μg/1 μl) was used for each transfection. Transfected MK3 cells were activated with 12 mM lithium chloride for 24 hours, and eGFP+ cells were isolated using flow cytometry at the Flow Cytometry Cell Sorting core at Northwestern University on a BD FACSAria SORP system and the BD FACSymphony S6 SORP system (BD, Franklin Lakes, NJ).

Luciferase Assay

M15 cells were grown to 70%–85% confluence and were transferred with Tcf21_Flag empty vector (pcDNA3; Addgene), Tcf21_Flag mutant or WT plasmid generated and validated in our laboratory, TCF/LEF luciferase reporter (M50 Super 8× TOPFlash, plasmid #12456; Addgene), and β-galactosidase plasmid as a measure of transfection efficiency using electroporation as described above. Transfected cells were incubated overnight and then treated with LiCl (15 mM) for 8 hours and lysed with reporter lysis buffer. The luciferase expression was assessed using the Luciferase Reporter Assay System (E1500; Promega, Madison, WI) and a luminometer. β-Galactosidase was measured with the β-Galactosidase Enzyme Assay System (E2000; Promega). The luciferase expression was standardized with β-Gal expression levels.

Immunoprecipitation and Western Blot

MK3 cells were lysed with RIPA buffer (25 mM Tris-HCl, pH 7.6, 150 mM NaCl, 1% NP-40, 1% sodium deoxycholate, and 0.1% SDS), proteinase and phosphatase inhibitor cocktails (Protease Inhibitor Cocktail; p8340; Sigma–Aldrich), sodium orthovanadate, Phosphatase Inhibitor Cocktail #2 (P5726; Sigma–Aldrich) and Phosphatase Inhibitor Cocktail #3 (P0044; Sigma–Aldrich). After protein concentration measurement (BioRad Protein Assay Reagent cat. #500–0006), 1 μg of protein was used for each experiment. Tcf21 antibody (ab182134; Abcam) was added to the protein samples and incubated overnight at 4°C. Protein G agarose (50 μl; 11719416001; Sigma–Aldrich) was added to the samples and incubated for 90 minutes. Beads were pelleted by centrifugation and eluted with Laemmli sample buffer containing 5% of β-mercaptoethanol by boiling at 95°C for 5 minutes. The supernatant was collected after centrifugation and loaded on 7% SDS-PAGE, followed by Western blotting with Tcf21 (ab182134; Abcam) and β-catenin (ab2365; Abcam) antibodies, and probed with a polyclonal HRP secondary antibody (ab2365; Abcam).

Affymetrix Microarray and Bioinformatic Analysis

Gene-expression microarray analysis on total RNA extract from glomeruli of $Tcf21^{lacZ/lacZ}$ null mice at E18.5 was conducted using Mouse Affymetrix GeneChips 430–2.0

at the microarray facility in the Center for Applied Genomics (The Hospital for Sick Children, Toronto, Canada) (19). Four thousand genes whose expression was either up- or downregulated at least two-fold between $Tcf21^{lacZ/lacZ}$ null and WT samples were chosen for further analysis.

To determine the enrichment of specific lineage genes among those differential in the global Tcf21 KO, we counted the overlap with the each of the top 50 cell type markers that were previously reported (20). Significance of the overlap was calculated by comparing with the random distribution of overlaps achieved through permuting the marker labels. This was done independently for increased and decreased genes, and then the *P* value cutoff for a family-wise error rate of 0.05 was calculated using the Bonferroni correction for multiple hypotheses.

Statistical Analyses

Statistical analyses were carried out using GraphPad Prism v7 (GraphPad Software, San Diego, CA). Comparison of two groups was performed by two-tailed *t* test. A *P* value <0.05 was considered significant. Error bars show ±SEM.

Results
Tcf21 in Foxd1+ Stromal Progenitors Is Required for Normal Formation of the Kidney Medullary Stroma in a Cell Autonomous Manner

Tcf21 is ubiquitously expressed in Foxd1-derived interstitial cells (9,21,22). Here, we utilized Foxd1-eGFP-Cre;Tcf21$^{f/f}$ mice or their WT littermates to investigate the role of Tcf21 in interstitial progenitors. Tcf21 mRNA detected by *in situ* hybridization is markedly reduced in the stroma of Foxd1-eGFPCre;Tcf21$^{f/f}$ starting at E14.5, confirming effective and specific Foxd1Cre-mediated Tcf21 excision as we have previously shown (supplemental figure 4 in Ide *et al.*) (17) and confirmed here by quantitative PCR (Supplemental Figure 1). We first affirmed that the Foxd1-eGFPCre does not have a significant effect on kidney morphology (Supplemental Figure 2). At E16.5, the medullary stroma zone is significantly smaller in the mutant kidney than in the WT control (Figure 1, A, A′, B, and B′). Additionally, the Foxd1Cre;Tcf21$^{f/f}$ kidney shows expansion of the CM (Six2+ cells) at E16.5 (Figure 1, C and C′, yellow dashed line; for more detail, see Supplemental Figure 3). At E18.5, the medullary stroma is significantly smaller in the mutant compared with the WT (Figure 1D, quantification Figure 1E), as quantified by expression of smooth-muscle actin α2 (Acta2), that normally marks interstitial cells in the outer segment of the inner medulla (9). The morphologic changes of the Foxd1Cre;Tcf21$^{f/f}$ kidney are less notable by hematoxylin and eosin at E12.5 and E14.5 (Supplemental Figure 4). However, immunostaining with the stromal marker slug (9) demonstrates significant reduction of the stromal space at E14.5 (Figure 2, A and A′, quantification Figure 2E). Although Foxd1 cells give rise to most of the stromal cells, their expression diminishes early and remains expressed in a small subset of cells, specifically in the nephrogenic zone and around the hilum of the kidney (5,23). In contrast to slug expression, which preferentially marks the medullary stroma, Foxd1 expression, detected

by the promoter-driven GFP expression, is not significantly decreased in the mutant kidney at E14.5 (Figure 2, B and B′) and is confined to the nephrogenic zone. This suggests that Tcf21 in interstitial progenitors is primarily required for development of the medullary stroma. This is also demonstrated at E16.5, where expression of slug and Acta2 are markedly reduced in the inner layers (Figure 2, C, C′, D, and D′). These findings suggest that Tcf21 in Foxd1+ cells is required for the formation of the medullary stroma cell autonomously. The expansion of the Six2+ cells in CM of the mutant kidney indicates that Tcf21 in Foxd1+ cells is required for normal development of the NPC noncell autonomously.

It was recently shown that the inner segment of the outer medulla of the stroma expresses genes important for DNA replication and functions as a transient zone for interstitial cell amplification (4). We have previously shown (17) and redemonstrated here (Supplemental Figure 5A) that the stromal Tcf21 KO kidney has lower Ki67 expression at P0 compared with the WT. Further, Foxd1-eGFP+ cells isolated from Foxd1-eGFPCre;Tcf21$^{f/f}$ at P0 are smaller and grow at a slower pace compared with cells isolated from WT controls (Supplemental Figure 5B). This suggests that the severe constriction of the medullary stroma in the mutant is a result of reduction in Foxd1+ cell proliferation due to a lack of Tcf21.

Stromal Tcf21 Is Required for Differentiation of Foxd1+ Cells and Development of the Endothelium

The mural cells of the renal vasculature are derived from Foxd1+ progenitors (24). We next asked whether deletion of Tcf21 in Foxd1+ cells affects mural cell development. Examination of the medullary stromal areas revealed that in addition to the marked reduction of Acta2 expression in interstitial cells (Figure 3, A and A′), a layer of Acta2+ cells surrounding the arterial wall of stromal Tcf21-deficient kidneys is mostly absent at E18.5 (Figure 3, B and B′), suggesting poor development of pericytes. When stained with the pericyte marker CD146, stromal Tcf21-mutant kidneys indeed show reduced CD146+ cells surrounding the arterial endothelium of interlobular arteries at E16.5 (Figure 3, C, C′, and G). The defect in pericyte development was also notable in the peritubular capillaries of the medullary stroma where fewer pericytes were observed in the stromal Tcf21-deficient kidney (Figure 3, D, D′, E, E′, F, and F′). These data suggest that Tcf21 is required, cell-autonomously, for normal differentiation of Foxd1+ progenitors to pericytes.

The endothelial progenitors are present in the embryonic kidney before arterioles are formed and marked by the proto-oncogene c-Kit and the SCL (2). Tcf21 is not normally expressed in endothelial cells (18,25). We next asked whether stromal Tcf21 affects the development of the endothelium. Immunostaining with the pan-endothelial marker CD31 shows distorted pattern of the arterial tree in the mutant, demonstrating disorganized, shorter, and thinner arterioles, displaying abnormal centripetal pattern at E15.5 (Figure 4, A and A′). Additionally, the mutant kidney shows abnormal vessel branching with aberrant ramification leading into the renal capsule at E15.5 (Figure 4, A and A′, arrow, Supplemental Figure 6, movies). At E18.5, the mutant
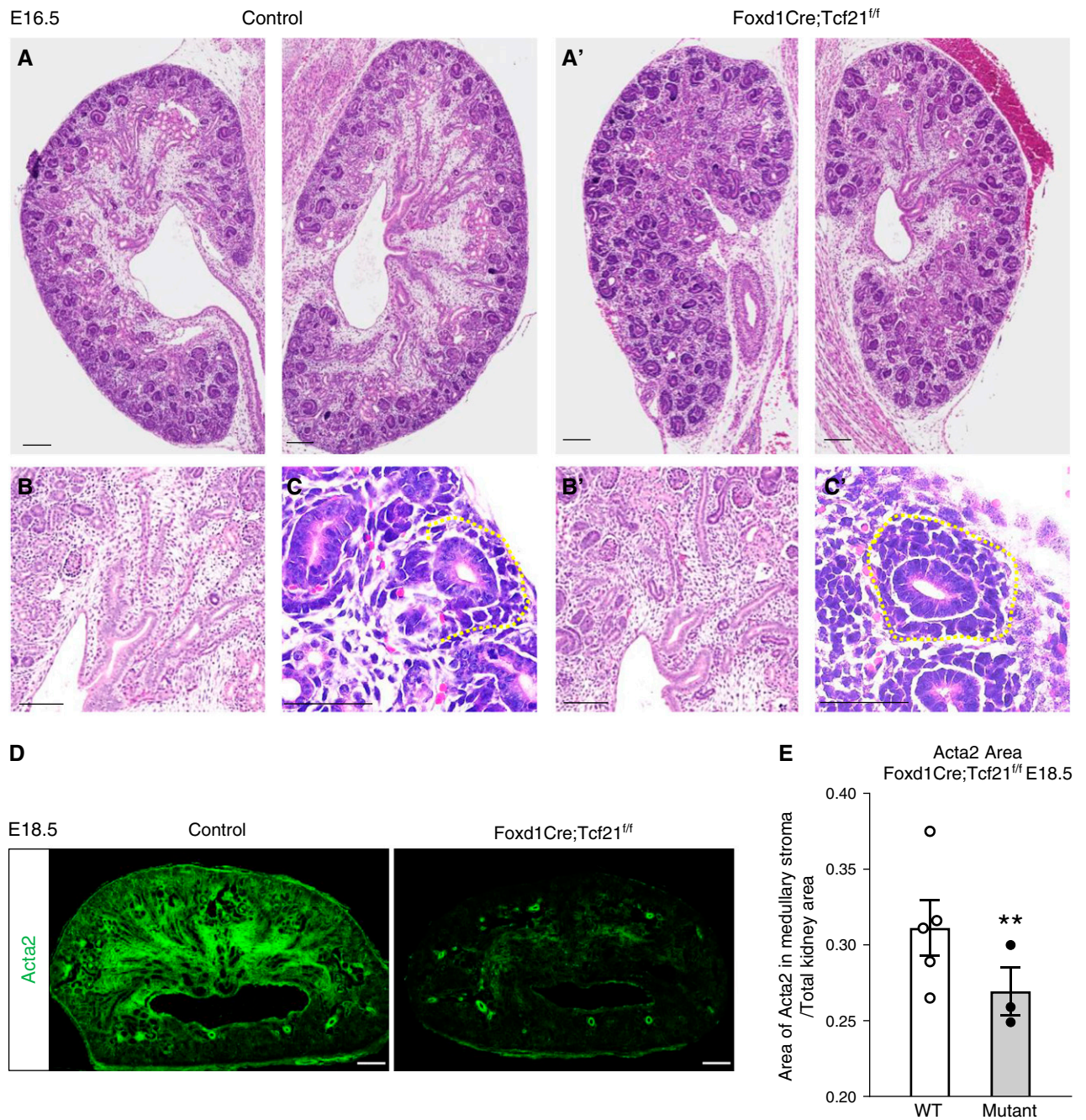
Figure 1. | Reduced medullary stroma in stromal Tcf21-deficient kidneys at E16.5 and E18.5. (A, A′, B, and B′) E16.5 kidneys of Foxd1Cre;Tcf21$^{f/f}$ mutants demonstrate reduced stromal space in the medullary compartment (hematoxylin and eosin staining). (C and C′) Expansion of the cap-mesenchyme domain containing the Six2+ nephron progenitor cells (yellow line). (D, D′, and E) E18.5 kidney of Foxd1Cre;Tcf21$^{f/f}$ shows severe reduction of smooth-muscle actin α 2 (Acta2) expression in the medullary stroma (immunostaining and quantification). Figures provided are representative images from three kidneys from at least two different litters. Scale bar 100 μm; **P<0.03.

arterial tree has fewer vessels globally (Figure 4B). This abnormal pattern is suggestive of immature vessels with fewer layers of smooth-muscle cells, and reminiscent of the Foxd1 KO murine kidney (24). At E16.5, examination of specific renal vascular beds shows that in addition to smaller interlobular arteries (Supplemental Figure 7), the mutant kidney demonstrates disrupted peritubular capillaries in the medulla (Figure 4, D–F) and simplified glomerular capillary loops (Figure 4, H, H′, and C). The number and size of the glomeruli are not significantly different in the mutant at E16.5 and E18.5 (Supplemental Figure 8), but there are fewer capillary loops (Figure 4C, Supplemental Figure 9). CD146+ mesangial cells in glomeruli are markedly reduced in the mutants (Figure 4, G, G′, and J, circled areas). The latter
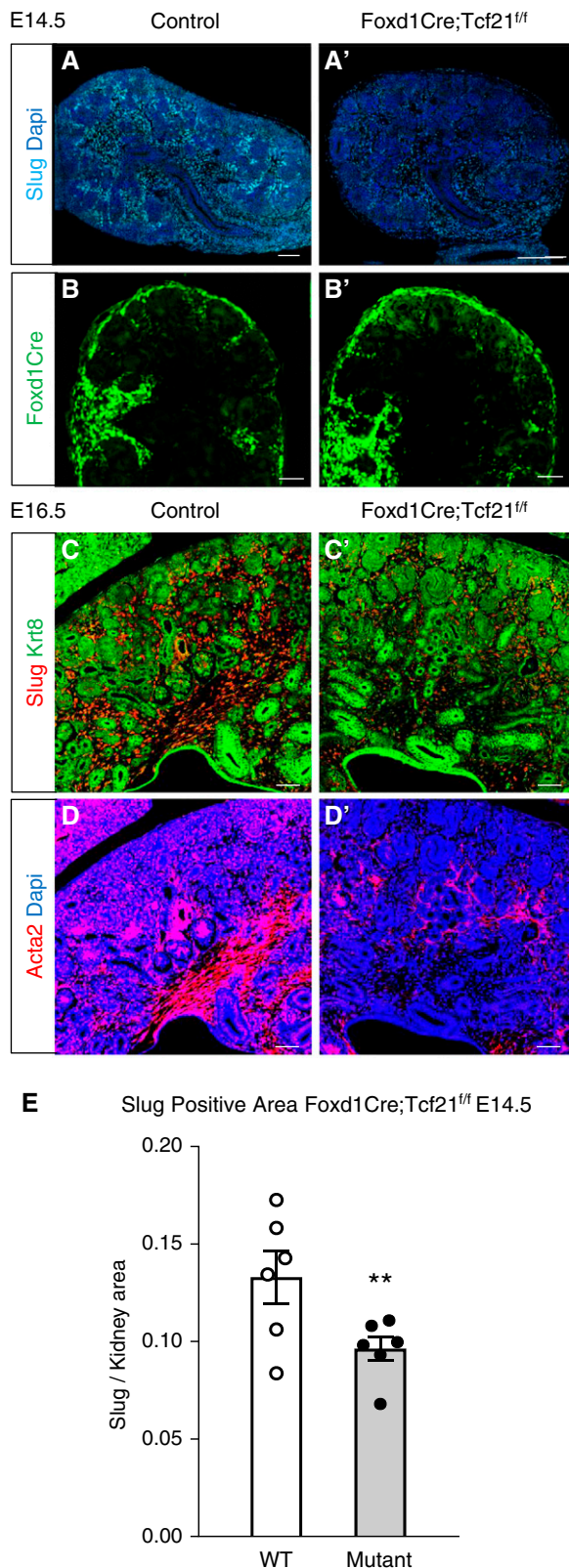
E14.5   Control   Foxd1Cre;Tcf21$^{f/f}$

A   A'

Slug Dapi

B   B'

Foxd1Cre

E16.5   Control   Foxd1Cre;Tcf21$^{f/f}$

C   C'

Slug Krt8

D   D'

Acta2 Dapi

E   Slug Positive Area Foxd1Cre;Tcf21$^{f/f}$ E14.5

Slug / Kidney area

**

WT   Mutant

Figure 2. | Stromal marker expression in stromal Tcf21-deficient kidneys at E14.5 and E16.5. (A and A′) Slug expression is diminished in Foxd1Cre;Tcf21$^{f/f}$ kidneys at E14.5 compared with the wild type (WT; immunostaining). (B and B′) In contrast, the expression of Foxd1 (evaluated by staining for GFP in Foxd1-eGFP-Cre;Tcf21$^{f/f}$ and Foxd1-eGFPCre;Tcf21$^{f/+}$) is not changed in the

finding is further confirmed by a decrease in PDGFRβ+ mesangial cells in Tcf21 stromal mutants (Supplemental Figure 10). Together, these data suggest that stromal Tcf21 is required for the normal development of vascular mural cells, mesangial cells, and the renal endothelium.

Tcf21 Cooperates with β-Catenin to Promote Wnt Signaling in Kidney Stromal Mesenchyme

The Wnt-β-catenin axis plays critical roles in embryogenesis. In the kidney stroma, the canonical Wnt responsive TCF/LEF pathway was shown to be active in the inner stromal zones (9). The severe constriction of the stromal compartment we observed in the Foxd1CreTcf21$^{f/f}$ kidney is reminiscent of the Foxd1Cre;catnb$^{-/}$flox kidney where β-catenin is deleted under the control of the Foxd1 promoter (26). Thus, we hypothesized that the morphologic changes observed in the stromal Tcf21 KO kidney are mediated by disruption in β-catenin signaling. Using the MM murine cell lines MK3 and M15 (27,28), we examined the effect of Tcf21 on Wnt/β-catenin signaling. Immunostaining for β-catenin in Foxd1CreTcf21$^{f/f}$ kidneys showed markedly reduced expression in the medullary stroma at E14.5 and E16.5 (Figure 5, A, A′, B, and B′). Immunoprecipitation of Tcf21 in MK3 cells showed direct interaction between Tcf21 and β-catenin, in both the presence and the absence of β-catenin stabilization with LiCl$_2$ (Figure 5C).

In MK3 cells, β-catenin stabilization by LiCl$_2$ induced expression of the Wnt target genes Wnt4, Pla2g7, Pax8, Tafa5, and Cited1 in a dose-dependent manner (Figure 6A). Importantly, Tcf21 mRNA expression also increased after β-catenin stabilization, suggesting that Tcf21 expression is regulated by β-catenin. The NPC marker C1qdc2 is not a β-catenin target and did not change with LiCl$_2$ stimulation. Next, we examined if Tcf21 affects TCF/LEF promoter activity. Tcf21 overexpression in M15 cells significantly enhanced the responsive TCF/LEF reporter activity upon β-catenin stabilization with LiCl$_2$ (Figure 6B). In contrast, over-expression of Tcf21 in the basal state did not significantly enhance TCF/LEF promoter activity (Figure 6B). Finally, we evaluated the expression of the stromal Wnt target genes in kidney explants of stroma Tcf21 mutants and controls. Expression of Thy1 and Apcdd1 was lower in the mutant compared with the control (Figure 6C), further supporting that stromal Tcf21 regulates β-catenin signaling in the stroma. Interestingly, these Wnt target genes are equally induced in kidney explants of WT or Tcf21 mutant when incubated with CHIR, which strongly stabilizes β-catenin and bypasses Wnt-mediated β-catenin stabilization. Representative images of explants are shown in Figure 6D. Taken together, our findings support a model where Tcf21 enhances β-catenin signal by increasing the pool of β-catenin and promote stromal cell proliferation and

Figure 2. | *Continued.* mutant. (C and C′) At E16.5, Slug expression is dramatically reduced in the medullary stroma in the stromal Tcf21 knockout kidneys. (D and D′) The Acta2 is severely reduced in the interstitial cells in the medulla of the stromal Tcf21 knockout kidney. (E) quantification of Slug+ area normalized to total kidney area in Foxd1Cre;Tcf21$^{f/f}$ kidneys and WT control. Scale bar 100 μm; $P=0.03$.
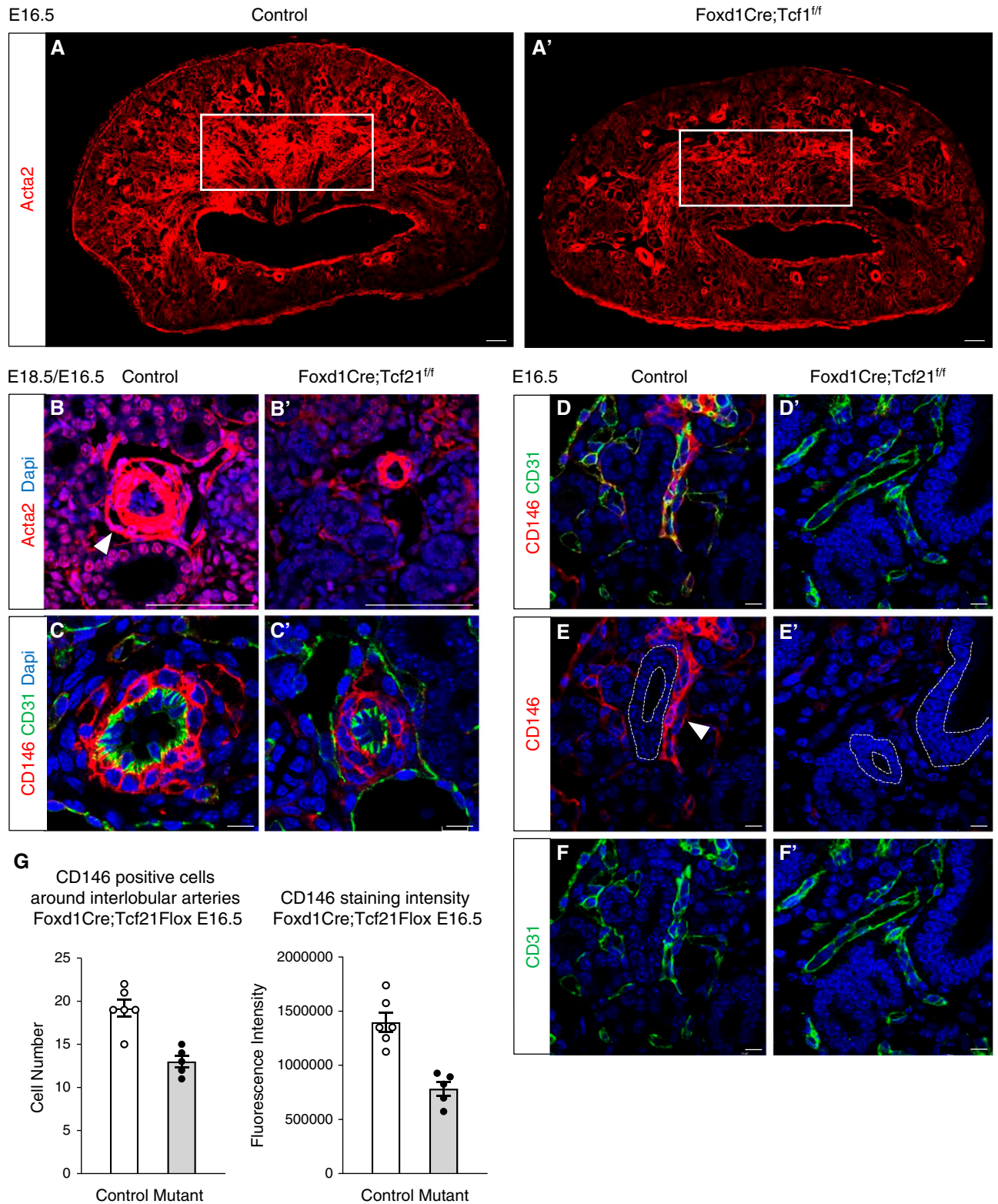
Figure 3. | Tcf21 is required for differentiation of Foxd1+ progenitors to smooth-muscle cells and pericytes. (A and A′) Reduction of Acta2 expression in interstitial cells at E16.5 (immunofluorescence). (B and B′) A layer of Acta2+ cells surrounding the arterial wall of stromal Tcf21-deficient kidneys is absent at E18.5. (C, C′, and G) Interlobular (corticoradial) arteries show reduced CD146+ pericyte cell number and expression in stromal Tcf21-mutant kidneys at E16.5. (D, D′, E, E′, F, and F′) Reduced expression of the pericyte marker CD146 surrounding the peritubular capillaries of the medullary stroma in Foxd1Cre;Tcf21$^{f/f}$ kidneys. Scale bar 100 μm; (C and C′) scale bar 10 μm.
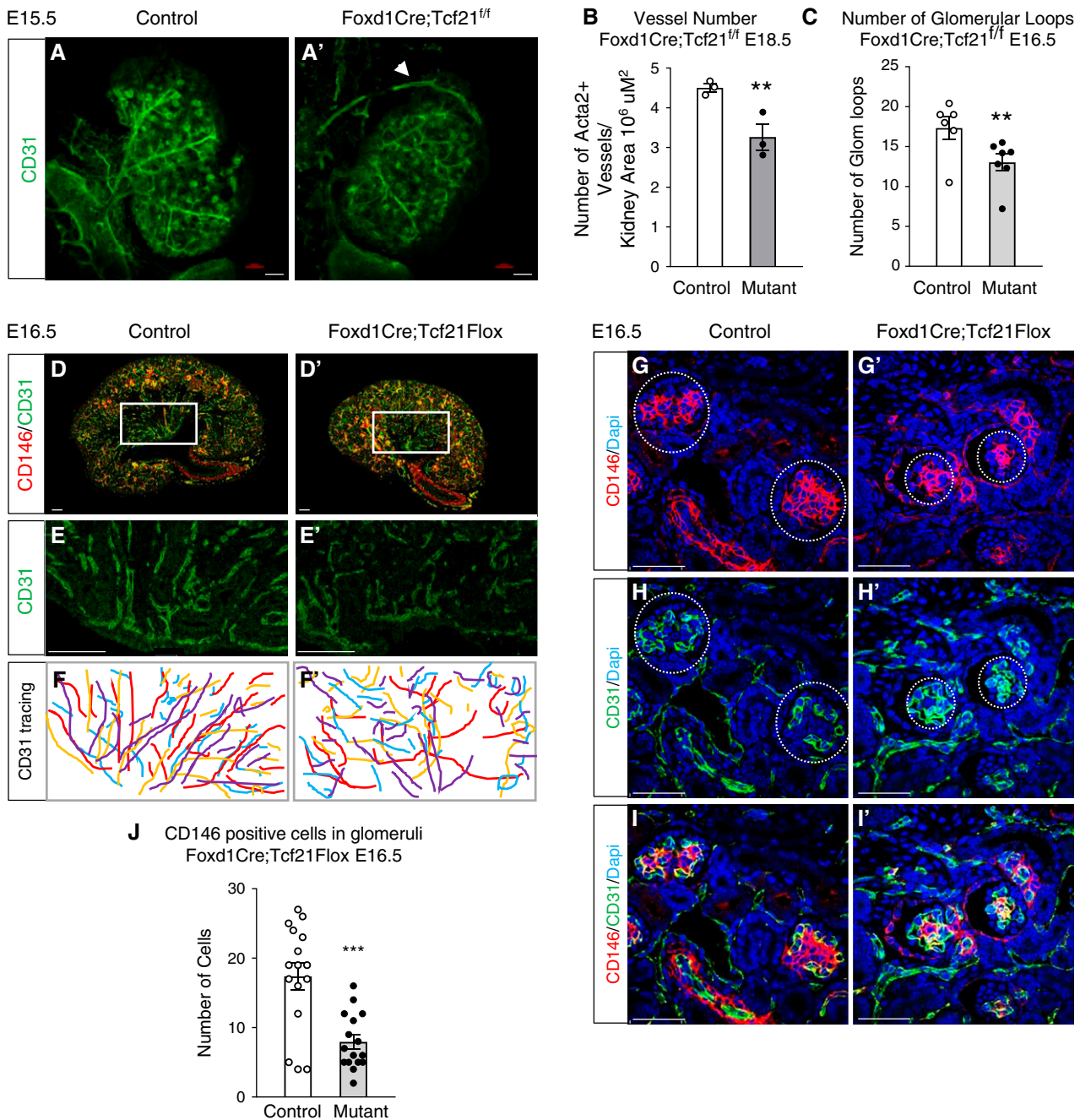
Figure 4. | **Stromal Tcf21 is required for normal development renal arterial tree.** (A and A′) CD31 expression demonstrates distorted renal arterial tree in Foxd1Cre;Tcf21$^{f/f}$ mutants at E15.5 (immunostaining). The mutant vessels are disorganized, shorter, and thinner, and display abnormal centripetal pattern. The arteries' branching pattern is abnormal, with aberrant ramification leading into the renal capsule (white arrowhead). (B) Quantification of vessel number of the stromal Tcf21 munt at E16.5 shows fewer vessels. (D, D′, E, and E′) E16.5 Foxd1-Cre;Tcf21$^{f/f}$ kidneys show disrupted peritubular capillaries in the medulla. (F and F′) Tracing of CD31+ peritubular capillaries in controls and mutants (n=4). (G, G′, and J) Reduced number of CD146+ mesangial cells in glomeruli (circled areas) in stromal Tcf21-deficient kidneys. (H, H′, and C) Simplified and fewer glomerular capillary loops capillary loops in mutants. Scale bar 50 μm; ***$P < 0.01$.

differentiation when the pathway is activated by Wnt ligands (Figure 7).

Discussion

Growing evidence indicates that the renal stroma is not solely a scaffold to the kidney but is active in directing kidney development (29–34). Here, we report that Tcf21 in Foxd1+ interstitial progenitors facilitate development of the medullary stroma. Stromal Tcf21 is required for differentiation of the stromal progenitors to their derivatives—the smooth-muscle cells, pericytes, and mesangial cells—and is essential for normal development of the renal endothelium and arterial tree. Our data suggest that Tcf21
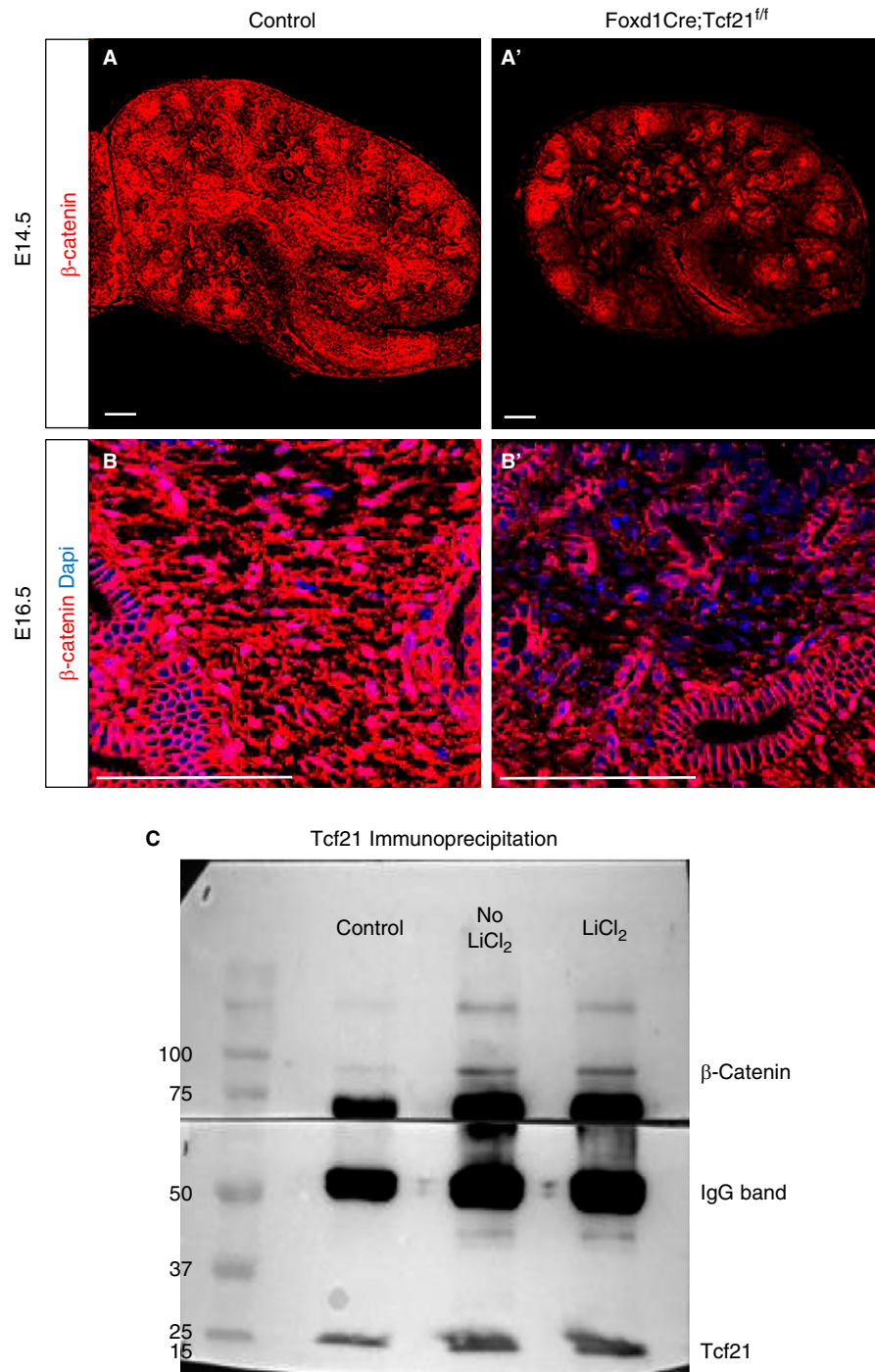
Figure 5. | Stromal Tcf21-deficient kidneys have lower β-catenin protein expression in the medullary stroma. (A, A′, B, and B′) β-Catenin protein expression is markedly reduced in the interstitium of the Foxd1Cre;Tcf21$^{f/f}$ kidney at E16.5 and E14.5 (immunostaining). (C and C′) Immunoprecipitation of Tcf21 of in MK3 cells showed direct interaction between Tcf21 and β-catenin, in both the presence and absence of β-catenin stabilization with LiCl$_2$. Scale bar 100 μm.

regulates stromal proliferation and that Tcf21 functions through β-catenin stabilization. Others have reported that stromal progenitors are more heterogeneous than previously appreciated (9). Indeed, in the Foxd1Cre;Tcf21$^{f/f}$ kidney, the effect of Tcf21 was most dramatic in the medulla, where interstitial cells proliferate, whereas milder changes were noted in the cortical stroma. Stromal Tcf21 is also necessary for normal development of the renal endothelium and arterial tree. This abnormal pattern is reminiscent of that of the Foxd1 KO mouse (24). Because Tcf21 is not normally expressed in endothelial cells (18), our findings suggest that stromal Tcf21 modulates proper differentiation of

A

B

C

D
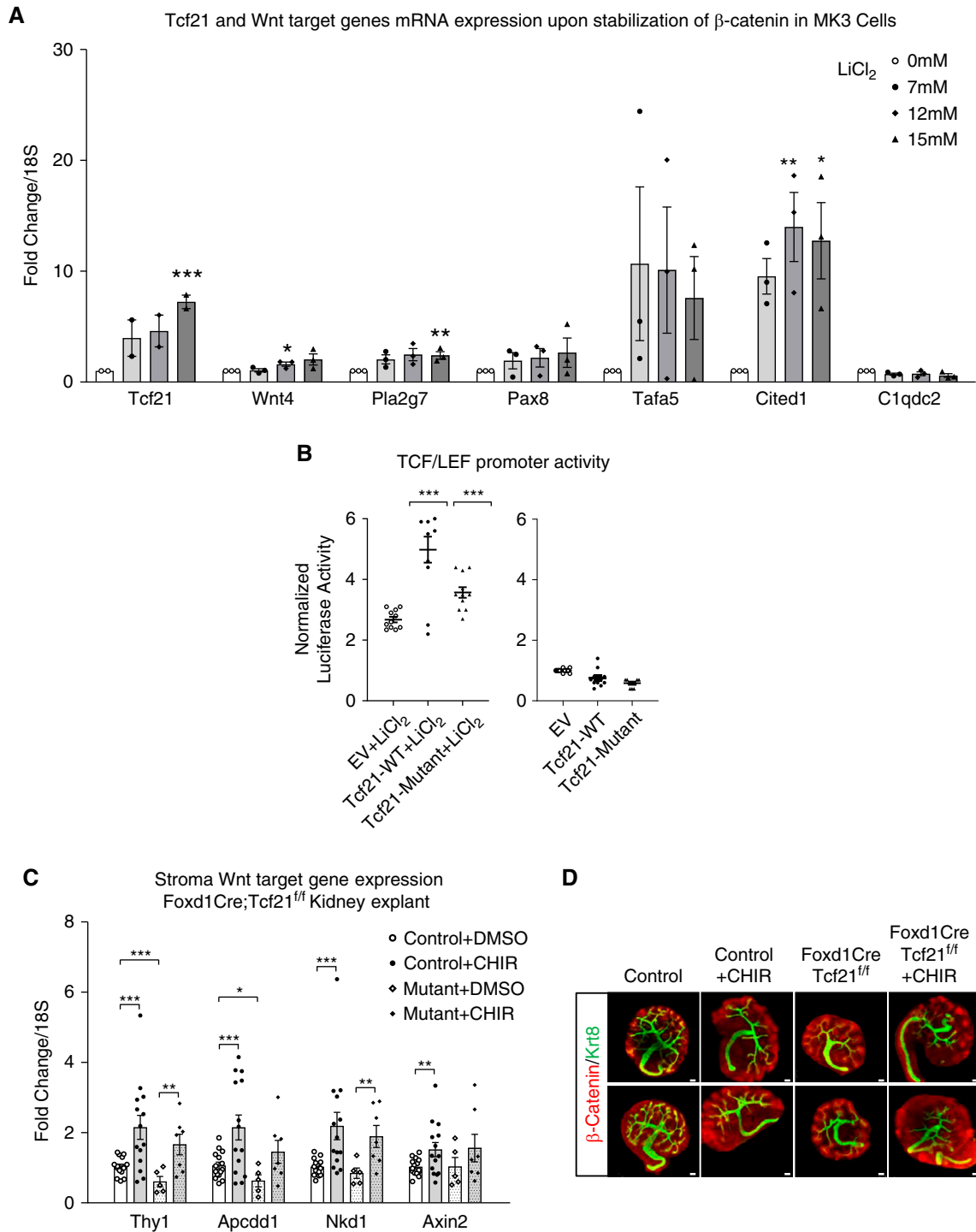
Figure 6. | Tcf21 enhances β-catenin action in metanephric mesenchymal cells. (A) In MK3 cells, β-catenin stabilization by $LiCl_2$ leads to an increase in Tcf21 and Wnt target-gene mRNA in a dose- and time-dependent manner. Tcf21 mRNA expression is also increased after β-catenin stabilization (quantitative RT-PCR). The NPC marker C1qdc2 is not a β-catenin target and did not change with $LiCl_2$ stimulation. (B) Tcf21 overexpression in M15 cells significantly enhanced the responsive TCF/LEF reporter activity upon β-catenin stabilization with $LiCl_2$. In contrast, overexpression of Tcf21 in the basal state did not significantly enhance TCF/LEF promoter activity. (C) Expression of the stromal Wnt target genes Thy1, Axin2, Apccd1, and Nkd1 in kidney explants of stroma Tcf21 mutants and controls. Stromal Wnt gene expression is lower in the mutant compared with the control, whereas in kidney explants that were incubated with CHIR, activator of Wnt signaling, the expression of the stromal Wnt target genes was not reduced, further supporting that Tcf21 in Foxd1+ cells regulates β-catenin signaling in the stroma. Visualization of the experiment in (D). *$P<0.05$; **$P<0.03$; ***$P<0.01$ compared with no $LiCl_2$ and EV+$LiCl_2$, respectively.
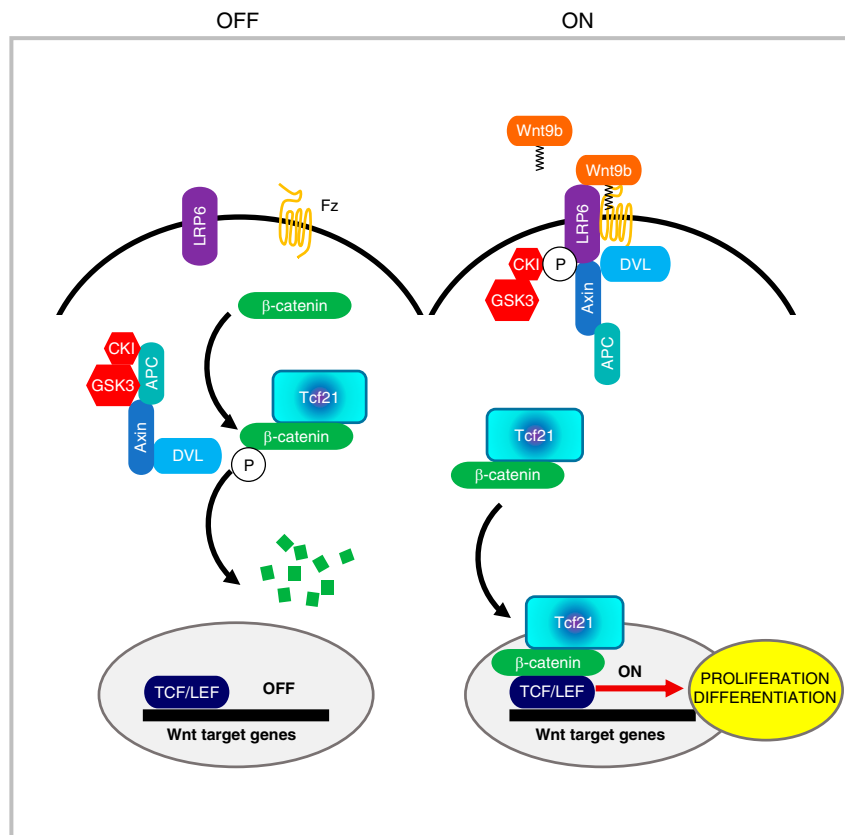
Figure 7. | Suggested model. In uninduced stromal progenitors (OFF state), Tcf21 binds β-catenin in the cytoplasmic destruction complex, preventing its degradation and thus facilitates β-catenin stabilization in the cytoplasm. Upon interstitial progenitor cell induction by Wnt9b (ON), Tcf21 accompanies β-catenin to the nucleus and enhances its transcriptional actions on TCF/LEF.

the interstitial progenitors, which is essential for vascular tree maturation.

The role of Tcf21 in progenitor cell differentiation and proliferation has been shown in other organs such as the heart (35–38). Here, we show that Tcf21 promotes Wnt/β-catenin signaling in the renal stromal mesenchyme. Specifically, we observed that Tcf21 is required for normal expression of β-catenin in the kidney, and that it binds to β-catenin in both basal and activated states, at least *in vitro*. Although Tcf21 interaction with β-catenin in the nucleus suggests transcriptional regulation, its interaction with β-catenin in the cytosol suggests a potential role in β-catenin stabilization.

It has been recently shown that the inner zones of the stroma express high levels of genes of the canonical Wnt-responsive TCF/LEF pathway (9). Additionally, evidence suggests that inactivation of β-catenin within Foxd1+ cells leads to severe constriction of the inner stromal regions (9,26). Our observation of lower β-catenin expression in the stromal Tcf21 mutants supports these data by ascribing an essential role for Wnt/β-catenin signaling in stromal development.

Wnt-ligand activation leads to stabilization of β-catenin and to its translocation to the nucleus where it facilitates TCF/LEF transcriptional activator actions. Tcf21 is a transcription factor that contains a bHLH domain that

mediates homo- or heterodimerization of transcription factors (39,40). Our observation that Tcf21 binds and enhances TCF/LEF promotor activity is in agreement with previous reports suggesting its binding to TCF protein family (41). In contrast, our observation that Tcf21 and β-catenin appear to interact in the cytoplasm is surprising and suggests that Tcf21 may be required to stabilize β-catenin and for its translocation into the nucleus. Others have reported enhancement of β-catenin nuclear translocation upon its binding to transcription factors, making interaction between Tcf21 and β-catenin plausible (42). However, our data do not address the mechanism by which Tcf21 regulates β-catenin.

In addition to the kidney, Tcf21 deficiency causes defective development of other organs (22,43), raising the possibility that Tcf21/β-catenin interaction is universal in embryogenesis. Together, our observations suggest a model where Tcf21 facilitates β-catenin stabilization in the cytoplasm and enhances β-catenin-mediated TCF/LEF transcriptional activation in the nucleus (Figure 7).

As to our observation of the noncell autonomous changes in stromal Tcf21 mutants (Supplemental Figure 4), these findings are in agreement with previous reports alluding to signaling from interstitial cells to NPC (8,32–34). Specifically, others reported Six2+ cell expansion in kidneys overexpressing β-catenin (Foxd1Cre;Catnb[ex3/+]) (44). Our

findings support these findings and suggest that the medullary stroma provides signals to the adjacent nonstromal lineages (32). Alternatively, the Foxd1+ progenitors may be less lineage restricted than currently thought, as has been suggested by others (24).

Lastly, while investigating the interaction between stroma and NPC, we utilized the Six2-Cre strain. However, we found that the kidneys of the Six2-Cre mouse are hypo-dysplastic and had smaller Cited1+ domain compared with the WT (Supplemental Figure 11). These findings raised concerns about using the Six2-Cre line and limited our ability to dissect Tcf21's action on NPC.

In summary, the findings reported here implicate Tcf21 in the development of the medullary stroma. Our data suggest that Tcf21 does so by regulating interstitial cell proliferation and differentiation *via* promoting β-catenin/TCF/ LEF signaling. The disrupted nephron epithelial structures adjacent to the medullary stroma in stromal Tcf21 KO highlights the importance of the stroma in normal nephron patterning.

Data Sharing Statement

All data are included in the manuscript and/or supporting information. Some previously published data were used for this study. The previously published data are clearly marked with appropriate references.

Supplemental Material

This article contains supplemental material online at https:// kidney360.asnjournals.org/lookup/suppl/doi:10.34067/KID.00055 72021/-/DCSupplemental.

Supplemental Table 1. Primer information.

Supplemental Figure 1. Tcf21 mRNA expression in Foxd1-eGFP-Cre;Tcf21^{f/f} kidney.

Supplemental Figure 2. Histology of the Foxd1Cre murine kidney.

Supplemental Figure 3. Noncell autonomous effects of stromal Tcf21.

Supplemental Figure 4. Hematoxylin staining ofTcf21 knockout (KO) kidneys at E12.5 and E14.5.

Supplemental Figure 5. Ki67 and cell growth of in stromal Tcf21-deficient kidneys.

Supplemental Figure 6. Abnormal arterial tree in stromal Tcf21 KO kidney (movies). Movie A: CD31 KRT8 E15.5 Foxd1Cre-Tcf21 Control x40. Movie A′: CD31 KRT8 E15.5 Foxd1Cre-Tcf21 Mutant x40. Movie B: CD31 E15.5 Foxd1Cre-Tcf21 control2. Movie B′: CD31 E15.5 Foxd1Cre-Tcf21 mutant2.

Supplemental Figure 7. Arterial diameter of Stromal Tcf21 KO kidneys.

Supplemental Figure 8. Glomerulus number and size in stromal Tcf21 KO kidney at E16.5.

Supplemental Figure 9. Glomerular phenotype of Stromal Tcf21 KO kidneys at E18.5.

Supplemental Figure 10. PDGFRβ expression in stromal Tcf21 KO kidneys.

Supplemental Figure 11. Histology of the Six2Cre murine kidney.

References

1. Grobstein C: Tissue disaggregation in relation to determination and stability of cell type. *Ann N Y Acad Sci* 60: 1095–1107, 1955 10.1111/j.1749-6632.1955.tb40091.x

2. Sequeira-Lopez MLS, Gomez RA: Renin cells, the kidney, and hypertension. *Circ Res* 128: 887–907, 2021 10.1161/CIRCRESAHA.121.318064

3. Boyle S, Misfeldt A, Chandler KJ, Deal KK, Southard-Smith EM, Mortlock DP, Baldwin HS, de Caestecker M: Fate mapping using Cited1-CreERT2 mice demonstrates that the cap mesenchyme contains self-renewing progenitor cells and gives rise exclusively to nephronic epithelia. *Dev Biol* 313: 234–245, 2008 10.1016/j.ydbio.2007.10.014

4. Kobayashi A, Valerius MT, Mugford JW, Carroll TJ, Self M, Oliver G, McMahon AP: Six2 defines and regulates a multipotent self-renewing nephron progenitor population throughout mammalian kidney development. *Cell Stem Cell* 3: 169–181, 2008 10.1016/j.stem.2008.05.020

5. Sequeira-Lopez ML, Lin EE, Li M, Hu Y, Sigmund CD, Gomez RA: The earliest metanephric arteriolar progenitors and their role in kidney vascular development. *Am J Physiol Regul Integr Comp Physiol* 308: R138–R149, 2015 10.1152/ajpregu.00428.2014

6. Humphreys BD, Lin SL, Kobayashi A, Hudson TE, Nowlin BT, Bonventre JV, Valerius MT, McMahon AP, Duffield JS: Fate tracing reveals the pericyte and not epithelial origin of myofibroblasts in kidney fibrosis. *Am J Pathol* 176: 85–97, 2010 10.2353/ajpath.2010.090517

7. Kobayashi A, Mugford JW, Krautzberger AM, Naiman N, Liao J, McMahon AP: Identification of a multipotent self-renewing stromal progenitor population during mammalian kidney organogenesis. *Stem Cell Reports* 3: 650–662, 2014 10.1016/j.stemcr.2014.08.008

8. Hatini V, Huh SO, Herzlinger D, Soares VC, Lai E: Essential role of stromal mesenchyme in kidney morphogenesis revealed by targeted disruption of Winged Helix transcription factor BF-2. *Genes Dev* 10: 1467–1478, 1996 10.1101/gad.10.12.1467

9. England AR, Chaney CP, Das A, Patel M, Malewska A, Armendariz D, Hon GC, Strand DW, Drake KA, Carroll TJ: Identification and characterization of cellular heterogeneity within the developing renal interstitium. *Development* 147: dev190108, 2020 10.1242/dev.190108

10. Kim JB, Pjanic M, Nguyen T, Miller CL, Iyer D, Liu B, Wang T, Sazonova O, Carcamo-Orive I, Matic LP, Maegdefessel L, Hedin U, Quertermous T: TCF21 and the environmental sensor aryl-hydrocarbon receptor cooperate to activate a pro-inflammatory gene expression program in coronary artery smooth muscle cells. *PLoS Genet* 13: e1006750, 2017 10.1371/journal.pgen.1006750

11. Lu X, Wang L, Chen S, He L, Yang X, Shi Y, Cheng J, Zhang L, Gu CC, Huang J, Wu T, Ma Y, Li J, Cao J, Chen J, Ge D, Fan Z, Li Y, Zhao L, Li H, Zhou X, Chen L, Liu D, Chen J, Duan X, Hao Y, Wang L, Lu F, Liu Z, Yao C, Shen C, Pu X, Yu L, Fang X, Xu L, Mu J, Wu X, Zheng R, Wu N, Zhao Q, Li Y, Liu X, Wang M, Yu D, Hu D, Ji X, Guo D, Sun D, Wang Q, Yang Y, Liu F, Mao Q, Liang X, Ji J, Chen P, Mo X, Li D, Chai G, Tang Y, Li X, Du Z, Liu X, Dou C, Yang Z, Meng Q, Wang D, Wang R, Yang J, Schunkert H, Samani NJ, Kathiresan S, Reilly MP, Erdmann J, Peng X, Wu X, Liu D, Yang Y, Chen R, Qiang B, Gu D; Coronary ARtery DIsease Genome-Wide Replication And Meta-Analysis (CARDIoGRAM) Consortium: Genome-wide association study in Han Chinese identifies four new susceptibility loci for coronary artery disease. *Nat Genet* 44: 890–894, 2012 10.1038/ng.2337

12. Maezawa Y, Onay T, Scott RP, Keir LS, Dimke H, Li C, Eremina V, Maezawa Y, Jeansson M, Shan J, Binnie M, Lewin M, Ghosh A, Miner JH, Vainio SJ, Quaggin SE: Loss of the podocyte-expressed transcription factor Tcf21/Pod1 results in podocyte differentiation defects and FSGS. *J Am Soc Nephrol* 25: 2459–2470, 2014 10.1681/ASN.2013121307

13. Gooskens SL, Gadd S, Guidry Auvil JM, Gerhard DS, Khan J, Patidar R, Meerzaman D, Chen QR, Hsu CH, Yan C, Nguyen C, Hu Y, Mulligan CG, Ma J, Jennings LJ, de Krijger RR, van den Heuvel-Eibrink MM, Smith MA, Ross N, Gastier-Foster JM, Perlman EJ: TCF21 hypermethylation in genetically quiescent clear cell sarcoma of the kidney. *Oncotarget* 6: 15828–15841, 2015 10.18632/oncotarget.4682

14. Maezawa Y, Binnie M, Li C, Thorner P, Hui CC, Alman B, Taketo MM, Quaggin SE: A new Cre driver mouse line, Tcf21/Pod1-Cre, targets metanephric mesenchyme. *PLoS One* 7: e40547, 2012 10.1371/journal.pone.0040547

15. Jain S, Suarez AA, McGuire J, Liapis H: Expression profiles of congenital renal dysplasia reveal new insights into renal development and disease. *Pediatr Nephrol* 22: 962–974, 2007 10.1007/s00467-007-0466-6

16. Richards KL, Zhang B, Sun M, Dong W, Churchill J, Bachinski LL, Wilson CD, Baggerly KA, Yin G, Hayes DN, Wistuba II, Krahe R: Methylation of the candidate biomarker TCF21 is very frequent across a spectrum of early-stage nonsmall cell lung cancers. *Cancer* 117: 606–617, 2011 10.1002/cncr.25472

17. Ide S, Finer G, Maezawa Y, Onay T, Souma T, Scott R, Ide K, Akimoto Y, Li C, Ye M, Zhao X, Baba Y, Minamizuka T, Jin J, Takemoto M, Yokote K, Quaggin SE: Transcription factor 21 is required for branching morphogenesis and regulates the Gdnf-axis in kidney development. *J Am Soc Nephrol* 29: 2795–2808, 2018 10.1681/ASN.2017121278

18. Quaggin SE, Schwartz L, Cui S, Igarashi P, Deimling J, Post M, Rossant J: The basic-helix-loop-helix protein pod1 is critically important for kidney and lung organogenesis. *Development* 126: 5771–5783, 1999

19. Cui S, Li C, Ema M, Weinstein J, Quaggin SE: Rapid isolation of glomeruli coupled with gene expression profiling identifies downstream targets in Pod1 knockout mice. *J Am Soc Nephrol* 16: 3247–3255, 2005 10.1681/ASN.2005030278

20. Ransick A, Lindström NO, Liu J, Zhu Q, Guo JJ, Alvarado GF, Kim AD, Black HG, Kim J, McMahon AP: Single-cell profiling reveals sex, lineage, and regional diversity in the mouse kidney. *Dev Cell* 51: 399–413.e7, 2019 10.1016/j.devcel.2019.10.005

21. Quaggin SE, Vanden Heuvel GB, Igarashi P: Pod-1, a mesoderm-specific basic-helix-loop-helix protein expressed in mesenchymal and glomerular epithelial cells in the developing kidney. *Mech Dev* 71: 37–48, 1998 10.1016/s0925-4773(97)00201-3

22. Cui S, Ross A, Stallings N, Parker KL, Capel B, Quaggin SE: Disrupted gonadogenesis and male-to-female sex reversal in Pod1 knockout mice. *Development* 131: 4095–4105, 2004 10.1242/dev.01266

23. Naiman N, Fujioka K, Fujino M, Valerius MT, Potter SS, McMahon AP, Kobayashi A: Repression of interstitial identity in nephron progenitor cells by Pax2 establishes the nephron-interstitium boundary during kidney development. *Dev Cell* 41: 349–365.e3, 2017 10.1016/j.devcel.2017.04.022

24. Mohamed T, Sequeira-Lopez MLS: Development of the renal vasculature. *Semin Cell Dev Biol* 91: 132–146, 2019 10.1016/j.semcdb.2018.06.001

25. Cui S, Schwartz L, Quaggin SE: Pod1 is required in stromal cells for glomerulogenesis. *Dev Dyn* 226: 512–522, 2003 10.1002/dvdy.10244

26. Yu J, Carroll TJ, Rajagopal J, Kobayashi A, Ren Q, McMahon AP: A Wnt7b-dependent pathway regulates the orientation of epithelial cell division and establishes the cortico-medullary axis of the mammalian kidney. *Development* 136: 161–171, 2009 10.1242/dev.022087

27. Valerius MT, Patterson LT, Witte DP, Potter SS: Microarray analysis of novel cell lines representing two stages of metanephric mesenchyme differentiation. *Mech Dev* 112: 219–232, 2002 10.1016/s0925-4773(02)00008-4

28. Dickinson KK, Hammond LC, Karner CM, Hastie ND, Carroll TJ, Goodyer P: Molecular determinants of WNT9b responsiveness in nephron progenitor cells. *PLoS One* 14: e0215139, 2019 10.1371/journal.pone.0215139

29. Magella B, Adam M, Potter AS, Venkatasubramanian M, Chetal K, Hay SB, Salomonis N, Potter SS: Cross-platform single cell analysis of kidney development shows stromal cells express Gdnf. *Dev Biol* 434: 36–47, 2018 10.1016/j.ydbio.2017.11.006

30. Song R, Lopez MLSS, Yosypiv IV: Foxd1 is an upstream regulator of the renin-angiotensin system during metanephric kidney development. *Pediatr Res* 82: 855–862, 2017 10.1038/pr.2017.157

31. Lin EE, Sequeira-Lopez ML, Gomez RA: RBP-J in FOXD1+ renal stromal progenitors is crucial for the proper development and assembly of the kidney vasculature and glomerular mesangial cells. *Am J Physiol Renal Physiol* 306: F249–F258, 2014 10.1152/ajprenal.00313.2013

32. Das A, Tanigawa S, Karner CM, Xin M, Lum L, Chen C, Olson EN, Perantoni AO, Carroll TJ: Stromal-epithelial crosstalk regulates kidney progenitor cell differentiation. *Nat Cell Biol* 15: 1035–1044, 2013 10.1038/ncb2828

33. Hum S, Rymer C, Schaefer C, Bushnell D, Sims-Lucas S: Ablation of the renal stroma defines its critical role in nephron progenitor and vasculature patterning. *PLoS One* 9: e88400, 2014 10.1371/journal.pone.0088400

34. Hurtado R, Zewdu R, Mtui J, Liang C, Aho R, Kurylo C, Selleri L, Herzlinger D: Pbx1-dependent control of VMC differentiation kinetics underlies gross renal vascular patterning. *Development* 142: 2653–2664, 2015 10.1242/dev.124776

35. Qureshi R, Kindo M, Arora H, Boulberdaa M, Steenman M, Nebigil CG: Prokineticin receptor-1-dependent paracrine and autocrine pathways control cardiac tcf21[+] fibroblast progenitor cell transformation into adipocytes and vascular cells. *Sci Rep* 7: 12804, 2017 10.1038/s41598-017-13198-2

36. Lupu IE, Redpath AN, Smart N: Spatiotemporal analysis reveals overlap of key proepicardial markers in the developing murine heart. *Stem Cell Reports* 14: 770–787, 2020 10.1016/j.stemcr.2020.04.002

37. Acharya A, Baek ST, Huang G, Eskiocak B, Goetsch S, Sung CY, Banfi S, Sauer MF, Olsen GS, Duffield JS, Olson EN, Tallquist MD: The bHLH transcription factor Tcf21 is required for lineage-specific EMT of cardiac fibroblast progenitors. *Development* 139: 2139–2149, 2012 10.1242/dev.079970

38. Wirka RC, Wagh D, Paik DT, Pjanic M, Nguyen T, Miller CL, Kundu R, Nagao M, Coller J, Koyano TK, Fong R, Woo YJ, Liu B, Montgomery SB, Wu JC, Zhu K, Chang R, Alamprese M, Tallquist MD, Kim JB, Quertermous T: Atheroprotective roles of smooth muscle cell phenotypic modulation and the TCF21

39. Murre C, Bain G, van Dijk MA, Engel I, Furnari BA, Massari ME, Matthews JR, Quong MW, Rivera RR, Stuiver MH: Structure and function of helix-loop-helix proteins. *Biochim Biophys Acta* 1218: 129–135, 1994 10.1016/0167-4781(94)90001-9

40. Zhao Q, Wirka R, Nguyen T, Nagao M, Cheng P, Miller CL, Kim JB, Pjanic M, Quertermous T: TCF21 and AP-1 interact through epigenetic modifications to regulate coronary artery disease gene expression. *Genome Med* 11: 23, 2019 10.1186/s13073-019-0635-9

41. Miyagishi M, Hatta M, Ohshima T, Ishida J, Fujii R, Nakajima T, Fukamizu A: Cell type-dependent transactivation or repression of mesoderm-restricted basic helix-loop-helix protein, POD-1/Capsulin. *Mol Cell Biochem* 205: 141–147, 2000 10.1023/a:1007057611868

42. Luo Y, Li M, Zuo X, Basourakos SP, Zhang J, Zhao J, Han Y, Lin Y, Wang Y, Jiang Y, Lan L: β-catenin nuclear translocation induced by HIF-1α overexpression leads to the radioresistance of prostate cancer. *Int J Oncol* 52: 1827–1840, 2018 10.3892/ijo.2018.4368

43. Lotfi CFP, Passaia BS, Kremer JL: Role of the bHLH transcription factor TCF21 in development and tumorigenesis. *Braz J Med Biol Res* 54: e10637, 2021 10.1590/1414-431X202010637

44. Drake KA, Chaney CP, Das A, Roy P, Kwartler CS, Rakheja D, Carroll TJ: Stromal β-catenin activation impacts nephron progenitor differentiation in the developing kidney and may contribute to Wilms tumor. *Development* 147: dev189597, 2020 10.1242/dev.189597

disease gene as revealed by single-cell analysis. *Nat Med* 25: 1280–1289, 2019 10.1038/s41591-019-0512-5